

# Stranski-Krastanov mechanism of growth and the effect of misfit sign on quantum dots nucleation

J.E. Prieto<sup>1</sup> and I. Markov<sup>2\*</sup>

<sup>1</sup>*Centro de Microanálisis de Materiales, Dpto. de Física de la Materia Condensada, IFIMAC and Instituto Universitario “Nicolás Cabrera”, Universidad Autónoma de Madrid, 28049 Madrid, Spain*

<sup>2</sup>*Institute of Physical Chemistry, Bulgarian Academy of Sciences, 1113 Sofia, Bulgaria\**

(Dated: February 3, 2022)

The thermodynamics of the Stranski-Krastanov mode of epitaxial growth and the effect of the sign of the lattice misfit are discussed. The Stranski-Krastanov mode of growth represents a sequence of layer-by-layer or Frank-van der Merwe growth followed by the formation of three-dimensional (3D) islands or Volmer-Weber growth. The occurrence of both growth modes mentioned above is in compliance with the wettability criterion of Bauer. The positive wetting function required for the occurrence of the Volmer-Weber growth is originated by the vertical displacements of the atoms close to the edges of the two-dimensional (2D) islands as a result of the relaxation of the lattice misfit. The monolayer high islands become unstable against bilayer islands, bilayer islands in turn become unstable against trilayer islands, etc. beyond some critical islands sizes. Monolayer islands appear as necessary precursors of three-dimensional (3D) islands. The critical island size for mono-bilayer transformation increases steeply with decreasing lattice misfit and diverges at a critical value of the misfit. This value divides the regions of Frank-van der Merwe and Stranski-Krastanov modes in a phase diagram of coordinates wetting-misfit. The transformation of monolayer to multilayer islands takes place either by consecutive nucleation and growth of 2D islands (layer-by-layer transformation), or by nucleation and lateral (2D) growth of multilayer islands (multilayer 2D transformation). The former occurs in the case of “stiff” overlayer materials and mostly in compressed overlayers. The latter takes place in the case of “soft” materials like Pb and In, mostly in tensile overlayers. Tensile films show non-nucleation transformation compared with the nucleation-like behavior of compressed films.

## INTRODUCTION

In 1958 Ernst Bauer published his famous thermodynamic criterion for the classification of the mechanisms of epitaxial growth.[1, 2] He derived an expression for the equilibrium shape, given by the ratio  $h/l$  (height/width), of a cubic crystal on a foreign substrate in terms of the interrelation of the specific surface energies of the substrate  $\sigma_s$ , epilayer,  $\sigma$ , and the substrate-epilayer interface,  $\sigma_i$ . The change of the surface energy,  $\Delta\sigma = \sigma + \sigma_i - \sigma_s$  associated with the formation of the epilayer, represents in fact a measure of the wetting of the substrate by the film material. In the case of incomplete wetting,  $\Delta\sigma > 0$ , the growth proceeds by the formation and growth of separate three-dimensional (3D) islands, a mechanism for which Bauer coined the term Volmer-Weber (VW) growth.[3] When  $\Delta\sigma \leq 0$  and the lattice misfit is negligible, the height of the 3D island is equal to zero and two-dimensional (2D) islands form instead giving rise to layer-by-layer or Frank-van der Merwe (FM) growth.[4, 5] And finally, when  $\Delta\sigma < 0$  and the lattice misfit is non-zero the growth begins by the formation of a *wetting layer* consisting of a few monolayers-thick film followed by the growth of 3D islands on top. This is the well-known Stranski-Krastanov mode of growth.[6]

The equilibrium shape of a crystal on an unlike substrate had been earlier derived by Kaischew in 1950 in terms of the binding energies between two atoms of the

deposit (cohesion energy,  $\psi$ ) and between an atom of the substrate and an atom of the film (adhesion energy,  $\psi^{prime}$ ).[7, 8] Both expressions, due to Bauer and Kaischew, respectively, for the equilibrium shape are in fact identical.[9] The condition  $\psi' < \psi$  is equivalent to  $\Delta\sigma > 0$ ,  $\psi' = \psi$  corresponds to  $\Delta\sigma = 0$  and  $\psi' > \psi$  corresponds to  $\Delta\sigma < 0$ . It follows that the mechanism of growth depends on the interrelation of the cohesion and adhesion energies. As will be shown below, the lattice misfit plays a crucial role only when  $\psi' \geq \psi$  ( $\Delta\sigma \leq 0$ ). Note that the above conclusions about the mechanism of growth are based on the concept of the equilibrium crystal shape.

As shown by Rudolf Peierls, the mechanism of growth is closely connected with the sign of the derivative of the chemical potential with respect to the number of atoms in the overlayer,  $d\mu/dN$ . [10] As seen in Fig. 1, the VW growth is associated with  $d\mu/dN < 0$  and the FM growth requires the condition  $d\mu/dN > 0$ . This means that the VW growth is connected with a negative curvature,  $d^2G/dN^2 < 0$ , of the  $N$ -dependence of the Gibbs free energy of the thickening film, whereas the FM growth is connected with the opposite behavior,  $d^2G/dN^2 > 0$ . This implies that in the case of SK growth, the dependence of the Gibbs free energy on film thickness must possess an inflection point,  $N_i$ , at which the curvature of  $G$ ,  $d^2G/dN^2$ , changes sign from positive to negative with increasing film thickness. The analysis of the problem shows that the planar film is stable up to some crit-

ical thickness,  $N_{\text{cr}}$ , which is slightly smaller than  $N_i$ . At  $N = N_{\text{cr}}$   $\mu = \mu_{\infty}$  and  $P = P_{\infty}$  where  $\mu_{\infty}$  and  $P_{\infty}$  are the chemical potential and the equilibrium vapor pressure of the infinitely large bulk deposit crystal, respectively. Thus  $N_{\text{cr}}$  and  $N_i$  determine the thicknesses of the stable and unstable wetting layers, which are given in Fig. 1 by the lower dotted and the upper straight lines, respectively. Note that in the analysis of Peierls the dependences of the film Gibbs free energies on film thickness are smooth and differentiable, which results in  $\Delta\mu(N_{\text{cr}}) = 0$ . The analysis of Peierls leads to the same criterion as the one derived by Bauer  $\Delta\sigma = \sigma + \sigma_i - \sigma_s \geq 0$ . For more details the reader is referred to section 4.3.4 of Ref. (9).

It is obvious that the SK growth represents an instability of the planar growth against clustering owing to the accumulation of strain energy in the wetting layer. This led to the concept of nucleation of islands due to the trade-off between the cost of the additional surface energy of the 3D islands and the gain of energy due to the elastic relaxation of the 3D islands relative to the wetting layer[11–13]. Although this approach gives a valuable insight into the problem, it does not allow the determination of the mechanism of formation of the 3D islands on top of the wetting layer. The essence of the problem is that the coherent (dislocationless) SK mode consists of the formation of 3D islands of a material  $A$  on the same (strained) material  $A$ . [14]

On the other hand, Mo *et al.*[15] observed with the help of scanning tunneling microscopy (STM) Ge islands representing elongated pyramids (“hut” clusters) bounded by (105) facets. The authors suggested that the hut clusters are a step in the pathway to the formation of larger islands with steeper side walls.[16–18] The ways of relaxation of lattice misfit in the transition from hut clusters to larger islands with steeper side facets has been reviewed by Teichert.[19] Tersoff *et al.* have shown that the growth of SiGe superlattices up to 2000 layers resulted in a very narrow size distribution of the quantum dots.[20]. Chen *et al.*[21] and Vailionis *et al.* [22] studied the initial stages of formation of the hut clusters and found three- to four monolayers-high prepyramids with rounded bases in a narrow interval of Ge coverages. Sutter and Lagally [23] suggested another scenario for the formation of SiGe alloy clusters at low misfit. They observed by low-energy electron microscopy (LEEM) the formation of an array of stepped mounds (ripples) as precursors of the hut clusters. These ripples are inherent to strained films to relax the misfit strain as suggested by many authors.[24–27] Based on these observations, Sutter and Lagally suggested the concept of barrierless (nucleationless) formation of the 3D islands.[23] Similar views on the idea of barrierless transformation of the ripples into faceted islands were suggested by Tromp *et al.*[28] and by Tersoff *et al.*[29] The contradiction of the above-mentioned concepts of nucleation and nucleationless formation of 3D islands, as well as many other aspects of the growth modes

gave rise to intensive theoretical studies of the Stranski-Krastanov morphology by making use of both analytical approaches[31–33], and computer Monte Carlo[34–37] and molecular dynamics[38–41] simulations, and were debated in numerous review papers and monographs.[42–45]. However, among the most important questions remains the following: Is the nucleation concept of 3D clustering consistent with the wettability concept of Bauer?

In addition, the mechanism of growth of quantum dots in the SK mode depends strongly on the sign of the lattice misfit. In compressed overlayers the film atoms interact through the steeper repulsive branch of the interatomic potential, whereas in tensile overlayers the interaction through the weaker attractive branch prevails. The anharmonicity of the chemical bonding influences the adhesion of the 3D islands to the wetting layer or, in other words, the wettability as defined by Bauer, through the relaxation of strain both laterally (in-plane) and vertically (out-of-plane) at the steps forming the boundaries of the islands. This strain relaxation leads to two different mechanisms of 2D-3D transformation, the consecutive transformations of islands with gradually increasing height by nucleation of single monolayers, and a mechanism in which multilayer islands nucleate and then laterally (two-dimensionally) grow. Note that the two-dimensional multilayer islands grow only laterally keeping their height constant in contrast to three-dimensional islands which grow both in length and height.

The paper is organized as follows. In consecutive sections we consider the equilibrium vapor pressure of the 2D and 3D phases, the effect of lattice misfit on the film-substrate adhesion, the thickness of the stable wetting layer, the stability of mono- and multilayer islands, the layer-by-layer growth of 3D islands, and the multilayer growth of 3D islands. We then compare our findings with experimental data and discuss the results.

## EQUILIBRIUM VAPOR PRESSURE OF THE 2D AND 3D PHASES

In 1929 Stranski[46, 47] studied the stability of separate monolayers of a monovalent ionic crystal  $K^+A^-$  on the surface of the isomorphous divalent crystal  $K^{2+}A^{2-}$  by making use of the newly discovered concept of the half-crystal or kink position.[48–50] He found that the equilibrium vapor pressure of the first monolayer,  $P_1$ , is much lower than the equilibrium vapor pressure,  $P_0$ , of the bulk monovalent crystal. The reason is that the monovalent ions are attracted by the underlying divalent ions more strongly than by the corresponding monovalent ions of the same crystal. As the ions of the second monolayer are repulsed more strongly by the underlying divalent ions of the substrate crystal, its equilibrium vapor pressure will be higher than the equilibrium pressure  $P_0$ . The equilibrium vapor pressure of the third mono-

layer will be smaller than  $P_0$ , and that of the fourth monolayer will be already nearly equal to  $P_0$ , i.e. the energetic influence of the divalent substrate disappears beyond four monolayers. Thus they concluded that the chemical potential of a thin film of  $K^+A^-$  on  $K^{2+}A^{2-}$  varies with its thickness.

Ten years later Stranski and Krastanov extended the considerations of the same model by calculating the Gibbs free energies of formation of 2D nuclei of the first, second, third, etc., monolayers, as well as of two and four monolayers-thick 2D nuclei.[6] It turned out that 2D nuclei of the first monolayer can be formed at a vapor pressure  $P$  which is larger than  $P_1$ , but smaller than  $P_0$ . This means that the first monolayer can be deposited at *undersaturation* with respect to the bulk crystal for the reasons given above. The work of formation of 2D nuclei of the second monolayer is very large but that of 2D nuclei consisting of two monolayers belonging to the second and third level, (or in fact three-dimensional), is much smaller. The reason is that the chemical potential of a bilayer deposited on the first monolayer is lower than that of a single monolayer but still higher than  $P_0$ . It was found that the chemical potential of the bilayer is equal to the arithmetic average of the chemical potentials of the second monolayer (larger than the bulk chemical potential) and the third monolayer (slightly smaller than the bulk chemical potential). This means that the formation of doubly high 2D nuclei requires a *supersaturation*. Note that in the original study of Stranski and Krastanov the bilayer nuclei which form on the first stable monolayer are two-dimensional. This means that they should grow laterally and not as 3D islands in length and height.[51]

We now consider a crystal  $B$  with lattice parameter  $b$  on the surface of a crystal  $A$  with lattice parameter  $a$ . Contrary to the chemical potential,  $\mu_{3D}^0$ , of the bulk crystal  $B$ , the chemical potential of the thin film,  $\mu(n)$  will depend on the film thickness measured in number of monolayers  $n$  for two reasons: The first one is that the attraction of the atoms of the consecutive monolayers by the substrate decreases with increasing distance from the interface. A second source of dependence on the film thickness is the mechanism of relaxation of the lattice misfit, either by introduction of misfit dislocations, by alloying or by the film growing pseudomorphically with the substrate.

The dependence of the thermodynamic driving force  $\Delta\mu = \mu(n) - \mu_{3D}^0$  is shown in Fig. 1 as a function of the film thickness measured in number of monolayers.[52] These dependences follow from the detailed consideration of the thickness variation of the film chemical potential[9]

$$\mu(n) = \mu_{3D}^0 + a^2(\sigma + \sigma_i - \sigma_s) + \varepsilon_e(f) \quad (1)$$

where  $\varepsilon_e(f)$  is the homogeneous strain energy per atom stored in a separate monolayer of crystal  $B$  (we assume that the first layers wetting the substrate are equally strained), and  $f = (b - a)/a$  is the lattice misfit.

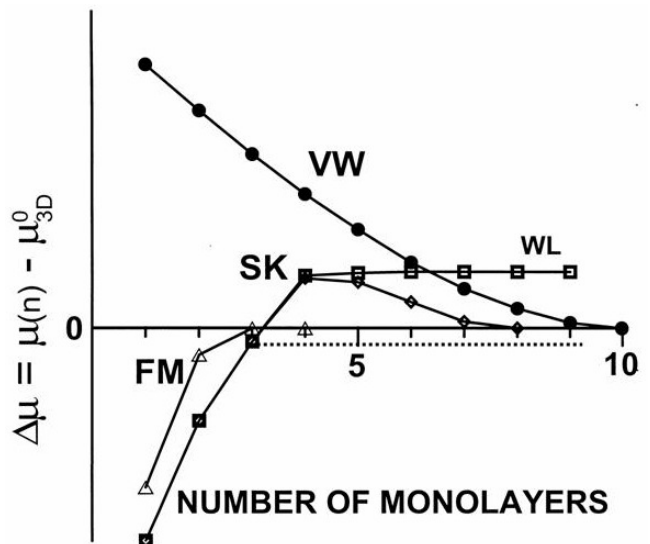


FIG. 1. Illustration of the dependence of the chemical potential of the overlayer on the film thickness in number of monolayers for the three modes of growth: Volmer-Weber (VW), Frank-van der Merwe (FM) and Stranski-Krastanov (SK). The upper straight line denoted by WL gives the chemical potential of the unstable wetting layer (a monolayer in excess which will be transformed into 3D islands), whereas the lower dotted line gives the chemical potential of the uppermost monolayer belonging to the stable wetting layer. (J. E. Prieto, I. Markov, Phys. Rev. B 66, 073408 (2002)). By permission of the American Physical Society.

Equation (1) can be written in the form

$$\Delta\mu = 2\sigma a^2\Phi + \varepsilon_e(f) \quad (2)$$

where

$$\Phi = \frac{\sigma + \sigma_i - \sigma_s}{2\sigma} = 1 - \frac{\beta}{2\sigma} \quad (3)$$

is the so called *wetting parameter* or *wetting function* with  $\beta$  the specific adhesion energy. In fact it is equal to the equilibrium aspect ratio  $h/l$  of a crystal on an unlike substrate.[1] In terms of binding energies the wetting parameter reads  $\Phi = 1 - \psi'/\psi$ . [7, 8] As noted above both expressions are identical.[9] Note that the expression for the wetting parameter given above is derived assuming that the lattice misfit does not affect the adhesion energy  $\beta$  ( $= \psi'/a^2$ ).

Let us now consider Fig. 1 in more detail. In the case of VW growth ( $\Phi > 0$ )  $\Delta\mu$  tends asymptotically to zero from above with increasing film thickness. The slope  $d\Delta\mu/dn$  is negative. In the case of FM growth ( $\Phi \leq 0, f \approx 0$ ),  $\Delta\mu$  tends asymptotically to zero with increasing film thickness from below. The slope  $d\Delta\mu/dn$  is positive. The third important case is  $\Phi < 0$  and  $f \neq 0$ . As long as the absolute value of  $2\sigma a^2\Phi$  in Eq. (2) is larger than  $\varepsilon_e(f)$ , the film will grow in a layer-by-layer

mode as in the FM case. As growth proceeds, the energetic influence of the substrate will diminish, and at some thickness the negative term  $2\sigma a^2\Phi$  will become smaller than the positive strain energy  $\varepsilon_e(f)$ .  $\Delta\mu$  will become positive and the next monolayer will become unstable against 3D islanding.

Let us now consider the problem in terms of equilibrium vapor pressures although the connection between the latter and the chemical potentials is straightforward ( $\mu \propto \ln P$ ). When  $\mu(1) < \mu_{3D}^0$  the first monolayer will be deposited at a vapor pressure higher than the equilibrium vapor pressure,  $P_1$ , of the first monolayer but smaller than the equilibrium vapor pressure,  $P_0$ , of the bulk crystal. The same is valid for all monolayers belonging to the stable wetting layer as long as  $\mu(n) < \mu_{3D}^0$ . It follows that stable monolayers including the uppermost one will be deposited at vapor pressures  $P_1 < P < P_0$  or, in other words, at *undersaturation* with respect to the bulk crystal. The deposition of 3D islands will take place at  $\mu(n) > \mu_{3D}^0$ , or at a *supersaturation* with respect to the bulk crystal.

Hence, in the case of the SK mode of growth, the equilibrium vapor pressure of the uppermost monolayer which belongs to the stable wetting layer (the dotted line in Fig. 1) is lower than the equilibrium vapor pressure,  $P_0$  of the bulk crystal, whereas the 3D islands on top are in equilibrium with a vapor pressure (the upper straight line denoted by WL in Fig. 1) which is higher than  $P_0$ . The dividing line is  $\Delta\mu = 0$  or  $P = P_0$ . At this pressure, the stable wetting layer cannot grow thicker and 3D islands cannot be formed. Material cannot be transferred from the stable wetting layer to the 3D islands as this implies an increase of the free energy of the system. Therefore it is thermodynamically unfavored. A planar film thicker than the stable wetting layer is unstable and the material in excess must aggregate into 3D islands upon annealing. We conclude that the wetting layer and the 3D islands are different phases in the sense of Gibbs (“homogeneous parts in a heterogeneous system”)[53] which can never be in equilibrium with each other.

### EFFECT OF LATTICE MISFIT ON THE FILM-SUBSTRATE ADHESION

It is instructive to consider first in some detail the one-dimensional model of Frank and van der Merwe of a finite chain of atoms in the sinusoidal potential field exerted by a rigid substrate.[4, 5] We will employ anharmonic bonds (steeper repulsion and weaker attraction branches of the interatomic potential) connecting the atoms instead of the harmonic approximation used by the authors.[54, 55] Such a consideration will give us valuable information concerning the coherent SK growth mode.

In the previous section we considered the wetting parameter and the lattice misfit as independent variables.

Frank and van der Merwe found that the end atoms in the chain are displaced from their sites in the bottoms of the potential troughs of the substrate. These displacements lead to two effects. First, the atoms close to the chain ends adhere more weakly to the substrate as compared with the atoms at the center, the chain as a whole loses contact with the wetting layer underneath and an effective positive wetting parameter results (Fig. 2). This appears as the thermodynamic driving force for the 2D-3D transformation. If all atoms are in the bottoms of the potential troughs, the wetting parameter will be precisely equal to zero and 3D islanding will be impossible. Note that if the chain is infinitely long the atoms will not be displaced and the wetting parameter will be again equal to zero. This is in fact the case for the monolayers belonging to the wetting layer.

Thus the finite 2D islands do not wet completely the substrate and at some critical size, they become unstable against bilayer or multilayer (3D) islands as discussed below. Note that beyond the wetting layer the energetic influence of the unlike substrate disappears and this makes the 2D-3D transformation possible. Such a transformation in the layers belonging to the wetting layer is impossible for thermodynamic reasons: the attraction of the atoms from the unlike substrate prevails over the strain energy per bond. Note also that the atoms in the tensile chain adhere more strongly to the wetting layer since more bonds are strained to fit it. On the contrary, bonds located further away from the ends in the case of compressed chains are also partially relaxed. Second, the bonds very close to the chain ends are maximally relaxed. If the chain consists of  $N + 1$  atoms connected by  $N$  bonds, the hypothetical 0-th and  $(N+1)$ -st bonds would be completely unstrained (Fig. 3).[5, 30, 54]



FIG. 2. Schematic representation of a finite crystal represented by the 1D chain model of Frank and van der Merwe.[4, 5]

We support our thermodynamic considerations by numerical calculations making use of a simple minimization procedure. We make use of two models. The first is the same atomistic model in 1+1 dimensions (length + height) as in Refs. (30) and (31) for fast qualitative calculations. The 3D islands are represented by linear chains of atoms stacked one upon the other. The island height is considered as a discrete variable which increases by unity starting from one. The second model is the more realistic (2+1)-dimensional construction [(length + width) + height]. The substrate (the wetting layer) in both cases is assumed to be rigid. In all cases we consider a crystalline film with an fcc lattice and (100) orientation at

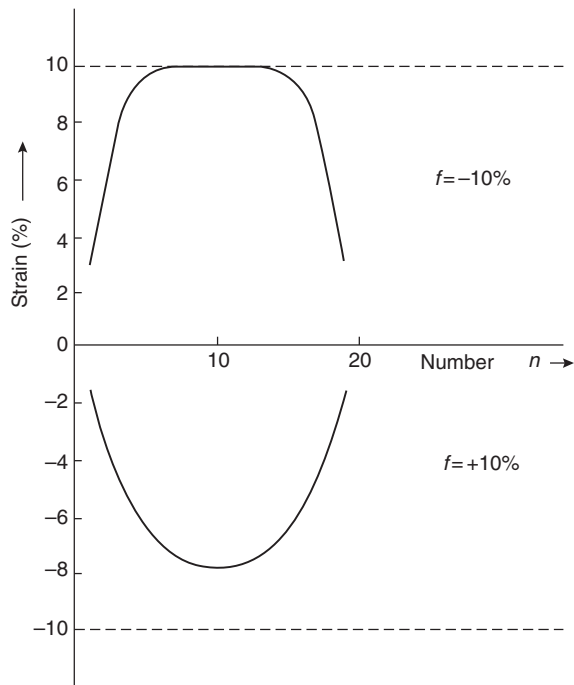


FIG. 3. Distribution of the strain in monolayer height compressed ( $f = 0.10$ ) and tensile ( $f = -0.10$ ) chains.

zero temperature. The atoms interact through an anharmonic pair-wise potential[56]

$$V(x) = V_0 \left[ \frac{\nu}{\mu - \nu} e^{-\mu(r-b)} - \frac{\mu}{\mu - \nu} e^{-\nu(r-b)} \right] \quad (4)$$

which, in spite of its simplicity, includes all necessary features to describe real materials (its strength and anharmonicity are governed by the constants  $\mu$  and  $\nu$ ,  $\mu > \nu$ ). In the case of  $\mu = 2\nu$  it turns into the familiar Morse potential. We consider interactions only in the first coordination sphere in order to mimic the directional bonds that are characteristic of elemental semiconductors.[57]

Let us emphasize once again that our system consists of a substrate crystal  $A$ , a stable wetting layer of crystal  $B$ , and 2D or 3D islands of crystal  $B$  on top of the wetting layer. When studying the formation of 3D islands on the wetting layer we consider the latter as a substrate. Thus we consider the growth of  $B$  on strained  $B$ . As we study the initial stages of the formation of 3D islands, they are assumed to be sufficiently small and coherent with respect to the wetting layer. In other words, we study the coherent (dislocationless) SK growth. In addition, we assume that the wetting layer is pseudomorphous with the substrate crystal  $A$ , i.e. the separate monolayers forming the wetting layer are equally strained and possess the same interatomic spacing as  $A$ .

Fig. 4 illustrates the differences (and similarities) between the coherent and incoherent (dislocated) SK growth modes. In the first case the end atoms are displaced vertically in the potential troughs of the substrate.

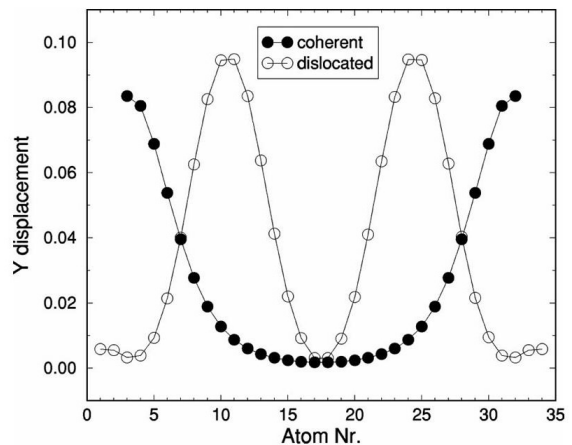


FIG. 4. Vertical displacements of the atoms of the base chain of a coherent ( $\bullet$ ) and a dislocated ( $\circ$ ), 3-monolayer-thick island. This is an illustration of the reduced adhesion of the islands to the wetting layer. The displacements are given in units of the lattice parameter of the wetting layer (which is equal to that of the substrate crystal) and are measured from the bottoms of the potential troughs of the wetting layer. The misfit  $f$  amounts to 7% and the islands contain 30 and 34 atoms in their base chains, respectively. (J. E. Prieto, I. Markov, Phys. Rev. B 66, 073408 (2002)). By permission of the American Physical Society.

In the second case the atoms in the cores of the dislocations are displaced in a similar way. As seen, in both cases the 3D islands (and the 2D islands as well, see above) lose contact with the substrate. Note that the dislocated island is a little bit longer (34 atoms) than the coherent one (30 atoms). This means that there is a critical size for the transformation of coherent into dislocated islands. The mean adhesion parameter  $\Phi$  increases with the island's height and saturates beyond several monolayers (Fig. 5). Here  $\Phi$  is calculated as the average adhesion energy of the atoms between the base chain and the wetting layer at the given value of the misfit minus the corresponding value for zero misfit. This is a very important result as it shows that thicker islands behave effectively as “stiffer” ones, i.e. with stronger interatomic bonds, as discussed below. This is directly connected with the multilayer mechanism of transformation of monolayer to multilayer islands.

Fig. 6 shows the dependence of the mean adhesion parameter on the lattice misfit in the case of coherent 3D islands. In fact, as discussed above, this is the dependence of the thermodynamic driving force for 3D island formation. As seen it is much larger in compressed islands than in tensile ones. The wetting parameter of tensile islands remains very small whereas that of compressed islands increases steeply for values of the lattice misfit beyond approximately 5%. The same qualitative results have been obtained in the case of a (2+1) dimensional model.[58]

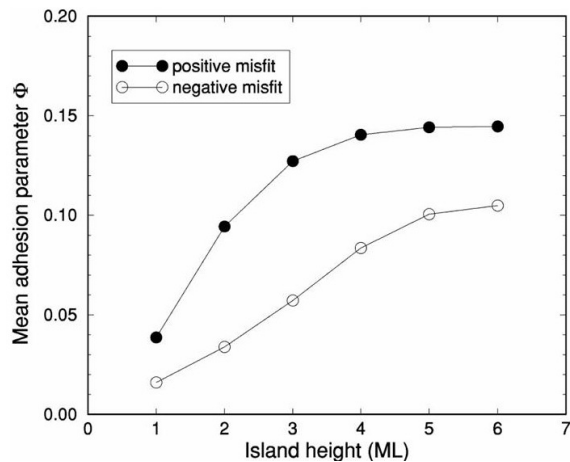


FIG. 5. Mean adhesion parameter  $\Phi$  as a function of the island height in number of monolayers for positive and negative values of the misfit of absolute value of 7%. The base chain consists of 14 atoms. (J. E. Prieto, I. Markov, Phys. Rev. B **66**, 073408 (2002)). By permission of the American Physical Society.

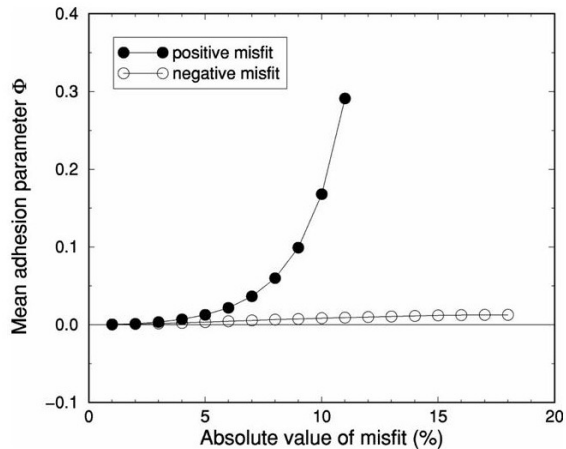


FIG. 6. Mean adhesion parameter of one monolayer thick coherent islands as a function of the lattice misfit. The islands consist of 20 atoms. Data for both compressed (●) and tensile (○) islands are shown in one and the same quadrant for easier comparison. (J. E. Prieto, I. Markov, Phys. Rev. B **66**, 073408 (2002)). By permission of the American Physical Society.

We conclude that the lattice misfit strongly affects the adhesion of the 3D islands on the strained wetting layer. The mean adhesion parameter and in turn the thermodynamic driving force for 3D island formation beyond the wetting layer are much larger for compressed islands than for tensile ones, for which  $\Phi$  remains close to zero. This means that tensile films display a much smaller tendency (if any) to Stranski-Krastanov growth as compared with compressed ones.

## THICKNESS OF THE STABLE WETTING LAYER

We can now write Eq. (1) in terms of the binding energies  $\psi$  (cohesion) and  $\psi'$  (adhesion) in the form

$$\mu(n) = \mu_{3D}^0 + \psi - \psi'(n) + \varepsilon_e(f) \quad (5)$$

where

$$\varepsilon_e(f) = 2G_b a^2 h f^2 \frac{1 + \nu_b}{1 - \nu_b} \quad (6)$$

is the energy of homogeneous strain per atom stored in each separate monolayer,  $h$  is the thickness of a monolayer and  $G_b$  and  $\nu_b$  are the shear modulus and the Poisson ratio of the crystal  $B$ , respectively. The contribution of the misfit dislocations is omitted since it is expected that they will be introduced at a thickness larger than that of the stable wetting layer.

We have to find the dependence of the adhesion energy  $\psi'(n)$  on the thickness  $n$ . This is a result of the decrease of the adhesion with the distance from the substrate surface. The first monolayer is most strongly attracted by the substrate, the second more weakly, the third very weakly, and the fourth monolayer most probably will not feel the presence of the substrate. Two types of  $\psi'(n)$  dependences are generally accepted; an inverse cubic  $n^{-3}$  dependence for van der Waals bonding (noble gases) and an exponential decay  $e^{-n/n_0}$  for metallic and covalent bonding in semiconductors.[59] It is worth noting that an empirical interatomic potential was devised for the properties of Si on the basis of a Morse-like pair-wise potential.[57]

The inverse cubic dependence  $n^{-3}$  follows from a pair-wise interaction of the Lennard-Jones 6-12 type between the adsorbate and the substrate[60, 61]

$$\psi'(n) = \psi - \frac{\psi - \psi'_1}{n^3} \quad (7)$$

where  $\psi'_1$  is the energy of desorption of an atom belonging to the first monolayer of the wetting layer from the unlike substrate at a coverage tending to zero.

Combining Eqs. (5), (6) and (7) under the condition  $\mu(n) = \mu_{3D}^0$  gives for the thickness of the stable wetting layer

$$n = \left( \frac{\psi}{\varepsilon_e} |\Phi| \right)^{1/3} \quad (8)$$

where the absolute value,  $|\Phi|$ , of the wetting parameter must be taken.

In the case of an exponential decay of the influence of the substrate, the thickness of the stable wetting layer reads[59]

$$\frac{n}{n_0} = \ln \left( \frac{\psi}{\varepsilon_e} |\Phi| \right) \quad (9)$$

where  $n_0$  is a parameter of order unity that can be determined by comparison with experiments.[59]

It is of interest to compare both expressions for  $n$ . In the case of deposition of Ge on Si(001)  $\varepsilon_e = 0.035$  eV/atom with  $G_{\text{Ge}} = 5.64 \times 10^{11}$  dyne/cm<sup>2</sup>,  $\nu = 0.2$ ,  $a = 3.84\text{\AA}$ ,  $h = 1.4\text{\AA}$  and  $f = 0.041$ . Assuming that the Ge atoms belonging to the first monolayer are attracted by the Si substrate with the same force as Si atoms (Ge and Si have similar chemical properties)  $\Phi = -0.216$ , and with  $\psi = 1.94$  eV (one half of the enthalpy of evaporation),  $\psi|\Phi|/\varepsilon_e = 12.0$ . We then obtain  $12^{1/3} = 2.3$ , and  $\ln 12 = 2.48$ . In other words we obtain two close values, similarly low when compared with the experimentally found value of 3 monolayers. This coincidence looks somewhat strange bearing in mind the different physics behind both expressions. In addition the parameter  $n_0$  remains unknown from the theoretical point of view.

The formulas above seem to imply that the thickness of the stable wetting layer tends to infinity when the lattice misfit and in turn the strain energy tend to zero. It is then noteworthy to mention that two reasons oppose this conclusion. First, as shown below, the 3D islanding is only possible at values of the misfit larger than some critical value. Even if this would not be the case, the decrease of the lattice misfit should lead to a transition from the Stranski-Krastanov mode to the Frank-van der Merwe mode of growth.

Let us consider a wetting layer consisting, say, of three equally strained monolayers, pseudomorphic with the substrate. The closer to the substrate, the more strongly a given monolayer is attracted by it. The decrease of the binding of each layer to the substrate is a discontinuous (step-like) function. It follows that the equilibrium vapor pressure of the consecutive monolayers (or the chemical potential) is an increasing step-like function of the number of monolayers but all these values are lower than the equilibrium vapor pressure of the bulk deposit crystal.[72] The growth of the next monolayer begins after the completion of the previous one as the chemical potential of the latter is smaller. Hence, each monolayer which belongs to the stable wetting layer is a distinct two-dimensional phase, and the formation of each new monolayer is a phase transition of first order.[59] Thus, in the particular case of Ge/Si(001) we have 4 Ge-containing phases, three separate monolayers belonging to the stable wetting layer plus the 3D islands, all four phases possessing different equilibrium vapor pressures.

We conclude that the thickness of the stable wetting layer increases as expected with increasing absolute value of the wetting parameter and with decreasing lattice misfit, but must remain always in the range of action of the interatomic forces, i.e., not more than 3-4 monolayers. Note that, as discussed above, the increase of the lattice misfit leads to an increase of the wetting parameter, so both parameters have opposite effects on the thickness of the wetting layer.

It follows from the above considerations that the number of the monolayers belonging to the stable wetting layer must be an integer. The thickness of the wetting layer has been determined in numerous papers as the thickness for the onset of 3D islanding. In all cases non-integer values have been established. Thus the values of 3.7 MLs in the case of Ge on Si(001),[73] 3.1-3.4 MLs in the case of Ge/Si(111),[74] 1.4 MLs[75] and 1.75 MLs[76] in the InAs/GaAs system, were measured from the onset of 3D islands formation. Borgi *et al.* found that the onset of 3D islanding depends both on the temperature and the substrate orientation in the case of deposition of InP on the (100) and (111)<sub>A,B</sub> surfaces of GaP.[77]

However, in all cases the amount of the material deposited in excess of the corresponding integer number of monolayers tends steeply to zero after the onset of formation of 3D islands.[73, 76] This unambiguously shows that the amount of deposit in excess is consumed by the 3D islands. Thus it is the integer number of monolayers that constitute the stable wetting layer. If we divide the excess material by the number of the 3D islands we can estimate the critical size of the monolayer islands which appear as precursors of the 3D islands, as shown below.

#### STABILITY OF MONO- AND MULTILAYER ISLANDS

Following the approach in Ref. (62) we plot the binding energies per atom of monolayer, bilayer, trilayer islands, etc., as a function of the total number of atoms making use of the more realistic (2+1)-D model.[58] Fig. 7 shows that the total energies of monolayer and bilayer islands under tensile stress are very close to each other irrespective of the larger absolute value of the misfit (-11%) compared with the corresponding behavior of compressed islands. Nevertheless, in both cases we observe a critical size,  $N_{12}$ , beyond which bilayer islands become energetically favored. Three-layer islands (not shown) become energetically favored beyond a critical size  $N_{23} > N_{12}$ , etc. Note that the crossover at positive misfit is much more pronounced in spite of the smaller absolute value of the misfit.

Thus we can expect that initially 2D islands are formed on the stable wetting layer, which beyond a critical size,  $N_{12}$ , become unstable against bilayer islands. The latter become unstable against trilayer islands beyond a critical size,  $N_{23}$ , etc. Thus the monolayer islands appear as necessary precursors of the 3D islands.[63, 64] Voigtländer and Zinner observed by STM that faceted 3D Ge islands are formed at the same locations on a Si(111) surface at which 2D islands were observed in the initial stage of deposition immediately after exceeding the critical thickness of the wetting layer.[65] Ebiko *et al.* found that the scaling function of the volume distribution of 3D InAs quantum dots on the surface of GaAs coincides with the

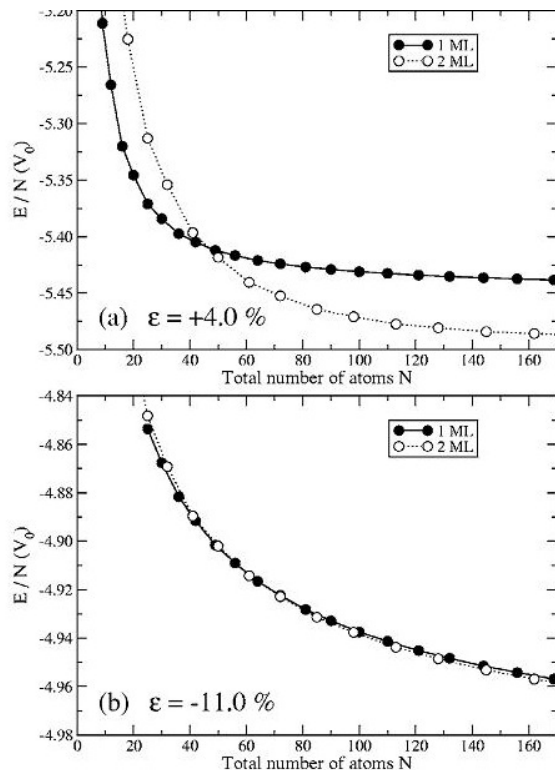


FIG. 7. Total energy per atom of mono- and bilayer islands at (a) positive and (b) negative values of the misfit as a function of the total number of atoms. The atoms interact through the potential (4) with  $\mu = 16$  and  $\nu = 14$ . (J. E. Prieto, I. Markov, Phys. Rev. B 72, 205412 (2005)). By permission of the American Physical Society.

scaling function for 2D submonolayer homoepitaxy with critical nucleus size  $i^* = 1$ . [66] Note that in submonolayer homoepitaxy the size of the 2D nucleus is defined as the compact stable cluster minus an atom and depends strongly on the temperature. Thus in the case of an fcc (100) surface the nucleus can consist of 3 atoms and the stable cluster of 4 atoms forming a square. [67] As will be shown below, the critical nucleus which gives rise to a new monolayer in the 2D-3D transformation, and the driving force for its formation is the lattice misfit, is defined in a different way. XXXX

It turns out that islands of a given thickness  $t$  are stable in an interval of sizes (in number of atoms) between  $N_{t-1,t}$  and  $N_{t,t+1}$ . We then plot for simplicity the critical size  $N_{12}$  for mono-bilayer instability, assuming that the bilayer islands can be considered as three-dimensional. Fig. 8 shows the dependence of the critical size  $N_{12}$  on the lattice misfit for the cases of compressive and tensile overlayers. The calculations are performed with the (1+1)D model. [52] A sharp increase with decreasing absolute value of the misfit is observed only in the case of compressed overlayers, where  $N_{12}$  clearly goes to infinity at some critical misfit  $f_{cr}$ . It is worth to note that in tensile overlayers the increase is less sharp and the curve is

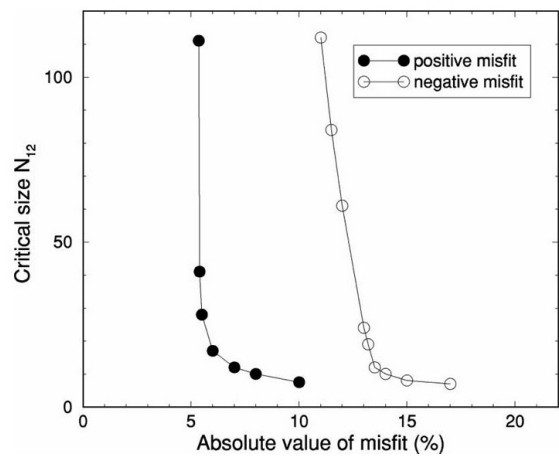


FIG. 8. The critical size,  $N_{12}$ , (in number of atoms) as a function of the lattice misfit for positive and negative values of the latter. The curves are calculated by making use of the (1+1)D model. (J. E. Prieto, I. Markov, Phys. Rev. B 66, 073408 (2002)). By permission of the American Physical Society.

displaced to larger absolute values of the misfit. We conclude that coherent 3D islands can be formed at misfits larger than  $f_{cr}$ .

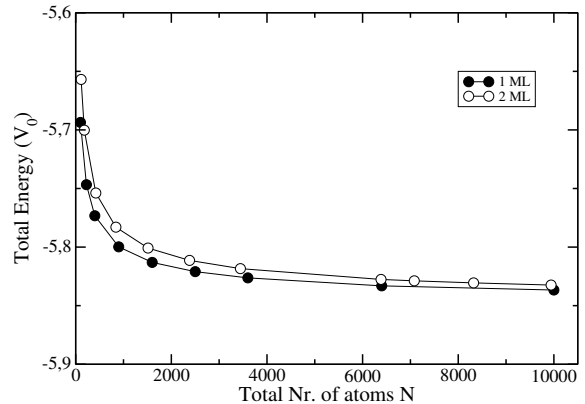


FIG. 9. Dependence of the energies of mono- and bilayer islands in (2+1)D for a misfit of 4%, smaller than the critical misfit  $f_{cr} = 5.2\%$ , ( $\mu = 2\nu = 12$ ).

For misfits smaller than  $f_{cr}$  the film is expected to continue growing in a layer-by-layer mode until misfit dislocations are introduced to relax the strain. This is clearly demonstrated in Fig. 9 which shows that monolayer islands in the (2+1)D model remain stable against bilayer ones up to a number of atoms as large as 10,000. The existence of a critical misfit for formation of coherent quantum dots does not allow the formation of a stable wetting layer thicker than the range of action of the interatomic bonding as discussed above.

Fig. 10 shows the misfit dependence of the critical island size  $N_{12}$  in the (2+1)D model. [58] Here, a new pa-



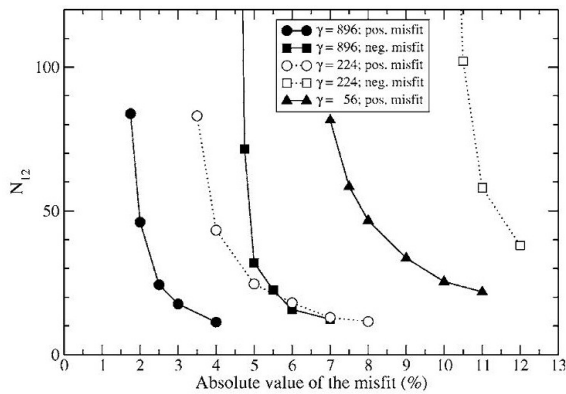


FIG. 10. Critical island size  $N_{12}$  as a function of the lattice misfit at different values of the force constant  $\gamma = \mu\nu V_0$ . The (2+1)D model and the potential (4) were used with  $\mu/\nu = 8/7$ . Coherent 3D islanding is favored in tensile epilayers only for “stiff” materials. (J. E. Prieto, I. Markov, Phys. Rev. B 72, 205412 (2005)). By permission of the American Physical Society.

parameter, the bond strength or the force constant of the interatomic bonds  $\gamma = \mu\nu V_0$ , is varied. Decreasing  $\mu$  and  $\nu$  in such a way that the ratio  $\mu/\nu$  is kept constant shifts  $N_{12}$  to larger absolute values of the misfit. This implies in practice the disappearance of  $N_{12}$ , since it shifts to unrealistically high values of the misfit at small values of  $\gamma$  in particular in tensile overlayers whereas  $N_{12}$  exists practically for all values of  $\gamma$  in compressed overlayers.

Another very important result is that in the case of an intermediate value of  $\gamma$  ( $\mu = 2\nu = 12$ ) the monolayer islands are always stable against bilayer islands ( $N_{12}$  disappears) but  $N_{13}, N_{14} \dots$  still exist, where  $N_{13}$  and  $N_{14}$  are the cross points of the energies of monolayer and three- and four-layer thick islands. At even smaller values of  $\gamma$  the critical values of  $N_{13}, N_{14} \dots$  consecutively disappear which leads to the idea of a novel mechanism of growth of the 3D islands which differs from the layer-by-layer growth. This mechanism should consist of a direct transformation of monolayer into multilayer islands by nucleation and lateral growth of two-dimensional multilayer islands on top of the initial monolayer islands. This transformation should take place at sizes greater than  $N_{1X}$ . Obviously this size should be much greater than  $N_{12}$ . We thus conclude that the 3D islands should form and grow by two distinctive mechanisms, one for “stiffer” and the other for “softer” materials. These two cases will be considered separately in more detail below.

### LAYER-BY-LAYER GROWTH OF 3D ISLANDS

The layer-by-layer mechanism of formation and growth of 3D islands was first suggested by Stoyanov and Markov[62] (see also Ref. 68) in the case of the VW growth of an elastically unstrained overlayer and was

further studied and applied to the case of strained heteroepitaxy.[30, 36, 58, 69] The rearrangement of mono- to bilayer islands, of bilayer to three-layer islands was established by Khor and Das Sarma by making use of Monte Carlo simulations in the (1+1)D case. During the deposition the process of 2D-3D transformation takes place in such a way that the bilayer islands are almost completely formed at the expense of the atoms incorporated into the monolayer islands, most of the atoms building the three-layers islands originate from the bilayer islands. [36] As shown above, this mechanism of growth is expected to take place in the case of “stiff” materials and in particular in compressed overlayers. We show that this behavior has the characteristics of a typical nucleation process but only in compressed epilayers.

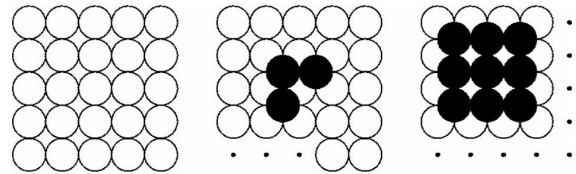


FIG. 11. Schematic representation of the process for the evaluation of the activation energy of the monolayer-bilayer transformation. The initial state is a square monolayer island. The intermediate state is a partial bilayer island whereas the final state is a truncated bilayer pyramid. (J. E. Prieto, I. Markov, Phys. Rev. B 72, 205412 (2005)). By permission of the American Physical Society.

For the study of the mechanism of mono-bilayer transformation, we simulate the following imaginary process. We consider an initial monolayer island with a square shape as shown in Fig. 11. We detach atoms from its edges and transfer them on top of the island thus building a compact second layer island at the center of the island underneath. The process proceeds until the second layer covers completely the first one thus producing a bilayer truncated pyramid. We calculate the energy associated to the mono – bilayer transformation by subtracting the energy of the initial monolayer island from the energy of the incomplete pyramid at every stage of the process.

Fig. 12 shows typical transformation curves of the energy change associated with the transfer of atoms from the lower to the upper level as a function of the number of atoms in the upper island for positive [Fig. 12(a)] and negative [Fig. 12(b)] values of the misfit. In compressed overlayers, the transformation curve for  $\Delta G$  exhibits the typical shape for the formation of the nucleus of a new phase. It displays a maximum,  $\Delta G_{\max}$ , for a critical cluster size,  $i^*$ , and then decreases beyond this size up to the completion of the transformation. The atomistics of the transfer process (i.e. the completion of rows in the upper level and their depletion in the lower one) are responsible for the non-monotonic behavior of the curve.

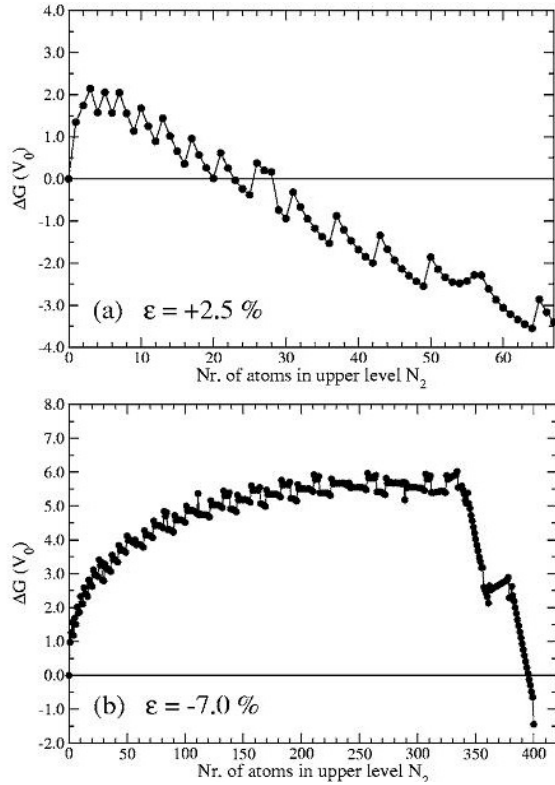


FIG. 12. Transformation curves showing the change of energy in units of the bond energy  $V_0$  as a function of the number of atoms in the upper level for (a) positive (+2.5%) and (b) negative (-7.0%) values of the misfit. The number of atoms in the initial monolayer island  $N_0 = 841 = 29 \times 29$  is chosen in a way to give a complete truncated bilayer pyramid consisting of  $21 \times 21 = 441$  atoms in the lower and  $20 \times 20 = 400$  atoms in the upper level;  $\mu = 2\nu = 36$  and the force constant  $\gamma = 648$ . (J. E. Prieto, I. Markov, Phys. Rev. B 72, 205412 (2005)). By permission of the American Physical Society.

Figure 13 demonstrates the dependence of the height of the barrier  $\Delta G_{\max}$  on the misfit in compressed and tensile overlayers. The figure at each point gives the number of atoms  $i^*$ . As seen  $\Delta G_{\max}$  decreases steeply with increasing misfit in a way similar to the decrease of the work required for nucleus formation with increasing supersaturation in the classical theory of nucleation.[9, 70, 71] We can accept a dependence of the form  $\Delta G_{\max} = Kf^{-n}$  where  $K$  is a constant proportional to the force constant  $\gamma$ , and  $f$  is the lattice misfit. Then we find  $n = 4.29$  for  $\mu = 2\nu = 12$  and  $n = 4.75$  for  $\mu = 2\nu = 36$ . It is worth noting that considering 3D nucleation on top of the wetting layer, Grabow and Gilmer predicted a value  $n = 4$  for small misfits (large nuclei) assuming  $\Delta G_{\max}$  is inversely proportional to the square of the supersaturation, which in turn is proportional to the square of the lattice misfit.[72] The same exponent of four was obtained also by Tersoff and LeGoues.[12]

Looking at Fig. 13 we note that the critical nuclei consist of a number of atoms which exceeds by one atom the

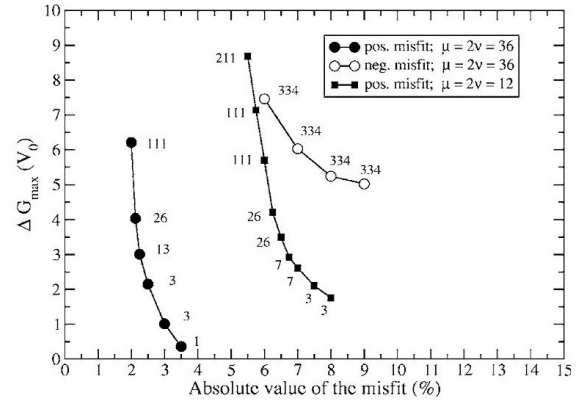


FIG. 13. Height of the energetic barriers in units of  $V_0$  as a function of the lattice misfit in compressed and tensile overlayers. The figures at each point show the number of atoms in the critical nucleus,  $i^*$ . The initial island size was  $29 \times 29 = 841$  atoms. (J. E. Prieto, I. Markov, Phys. Rev. B 72, 205412 (2005)). By permission of the American Physical Society.

size of a compact cluster. This is in accordance with the atomistic theory of nucleation where the critical nucleus size is given by  $i^* = i(i - 1) + 1$  ( $i = 1, 2, 3 \dots$ ).[78] The reason is easy to understand. The additional atom creates two kink positions for the growth of the next row of atoms. Thus, this additional atom can be considered as the one-dimensional nucleus which gives rise to a new atomic row and thus transforms the rectangular island into a square one. It is worth noting that one-dimensional nuclei cannot exist in the thermodynamic sense but can be defined by making use of a kinetic approach.[79–81] For a recent review see Ref. (9)

In the case of tensile overlayers, the transformation basically increases all the way up to a number of atoms which is approximately equal to the number of atoms required to complete the upper level minus the number of atoms necessary to build the last four edge rows of atoms. Thus the final collapse of the energy is due to the disappearance of 8 single steps which repulse each other and the formation of 4 low energy facets. The highest value of the number of atoms before the collapse of the energy does not depend on the misfit, and as a whole, the transformation curve displays a non-nucleation behavior. Having in mind that the maximum number of atoms in tensile overlayers is higher than that in compressed ones we can conclude that the process of 3D islanding will be very difficult as it will require (astronomically) very long times.

It is of interest to study the transformation to thicker islands. Figure. 14 shows the energies of transformation of mono- to bilayer islands, bilayer to three-layer island, and three- to four-layer islands. All curves have the characteristic behavior of a nucleation process. As shown in Ref. (62) the chemical potential of the upper island at

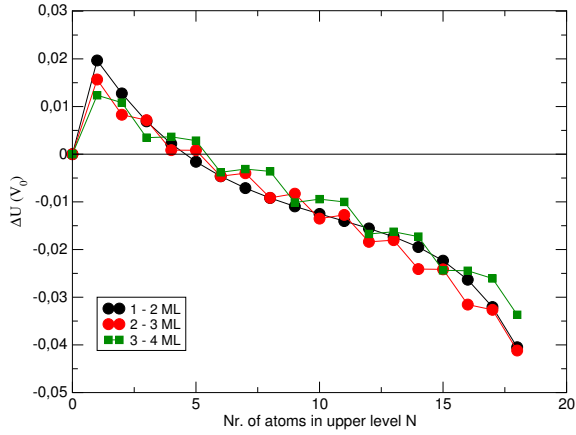


FIG. 14. (Color on-line) Energy change  $\Delta E_n$  in units of  $V_0$  connected with the transformation of mono- to bilayer islands (black circles), bi- to trilayer islands (red circles), and three- to four-layer islands (black squares), as a function of the number of atoms  $n$  in the uppermost chain.

the maximum is exactly equal to that of the initial monolayer island, and the supersaturation with which the nucleus of the second layer is in equilibrium is equal to the difference of the energies of desorption of the atoms from the like and the unlike substrate. This is, namely, the driving force for the 2D-3D transformation to occur. Note that the (1+1)D model is in fact one dimensional and the nuclei do not exist in the thermodynamic sense because the length of a row of atoms does not depend on the supersaturation as discussed above.[79–81] However, considering our (1+1)D model as a cross section of the real (2+1)D case, we can treat the curves in Fig. 14 as dependences of the free energy for nucleus formation and growth or, as consecutive transformation curves. We would like to emphasize that in the (2+1)D model the nucleus does not necessarily consist of one atom. Its size must depend on the lattice misfit, and in a real situation on the temperature. The curves describing the 2-3 and 3-4 transformations behave in the same way but the work for nucleus formation (the respective maxima) decrease with the thickening of the islands. This means that the mono-bilayer transformation is the rate-determining process for the total mono-multilayer (2D-3D) transformation.

### MULTILAYER GROWTH OF 3D ISLANDS

As mentioned in Section V in the case of negative misfits (tensile overlayers) a decrease of the force constant  $\gamma$  leads to the consecutive disappearance of the crossing points  $N_{12}, N_{13}, N_{14} \dots$ . As observed in Fig. 15 the reason is that the energy per atom of multilayer islands (in the particular case shown, of bilayer islands) remains always larger than that of monolayer islands.[82] The en-

ergy curves never cross, irrespective of the islands size. The energy curve for monolayer islands is crossed by the curve of the energy of the three-layer islands at a size  $N_{13}$ . The reason for the energy of the bilayer islands to be always larger than that of the monolayer islands is the weaker strain relaxation at the double step edge of the laterally smaller island of the same total number of atoms. The island must become of triple height in order for the strain relaxation to prevail over the step energy. This is in accordance with the considerations of van der Merwe *et al.*[83] Thicker island consisting of  $n$  layers have an effective force constant,  $\gamma_n$ , larger than the force constant,  $\gamma$ , of a single monolayer. Decreasing the material's stiffness (decreasing  $\gamma$ ) leads to the necessity of increasing the threshold thickness or, in other words, the effective force constant  $\gamma_n$ . This is shown in the inset in Fig. 15 which gives the dependence of the critical size  $N_{X-1}$  (beyond which single ML islands become unstable against X-ML islands) on the force constant  $\gamma$ . The critical thickness below which multilayer islands are energetically unfavored sharply increases, together with the critical volume, for decreasing force constant  $\gamma$ .

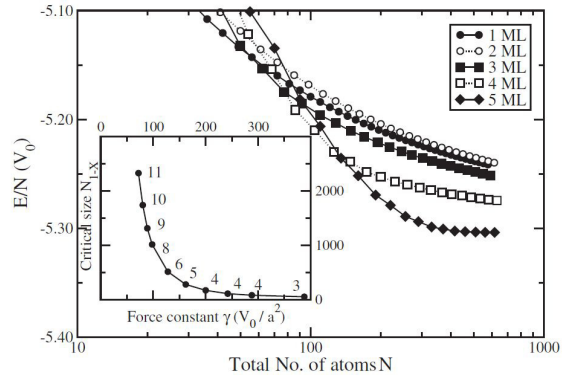


FIG. 15. Energy per atom of mono- and multilayer tensile islands as a function of the total number of atoms. The misfit amounts to  $-7\%$  and  $\mu = 2\nu = 26$ . The inset shows the dependence of the critical size  $N_{1-X}$  on the force constant  $\gamma$ .  $N_{1-X}$  is the size beyond which 1-ML islands become unstable against X-ML islands. The thickness X is denoted by the numbers at each point. (J. E. Prieto, I. Markov, Phys. Rev. Lett. 98, 176101 (2007)). By permission of the American Physical Society.

This is illustrated in Fig. 16. It shows a phase diagram of stability of mono- and multilayer islands in coordinates of island size  $N$  vs. strain energy per bond  $\mathcal{E} = 0.5\gamma f^2 a^2$ . The numbers in the plot give the heights of the stable islands inside the corresponding regions, limited by the curves shown. Single monolayer islands are stable at small numbers of atoms. Bilayer islands are stable at large strain energies i.e. at large force constant or large misfits. Otherwise, thicker islands will become stable. Islands thinner than a certain number of layers will be forbidden for thermodynamic reasons. Tensile overlay-

ers require larger absolute values of the misfit compared with compressed ones in order to compensate the weaker attractive forces between the atoms.

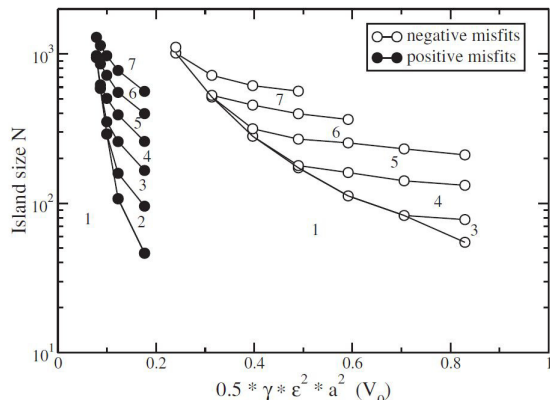


FIG. 16. Phase diagram in coordinates total number of atoms  $N$  vs. bulk strain energy per bond  $\mathcal{E} = 0.5\gamma f^2 a^2$ , for positive and negative values of the misfit and for potentials with  $\mu = 2\nu$ . The numbers mark the regions of stability of islands of the corresponding number of monolayers, regions which are limited by the displayed curves. [J.E. Prieto, I. Markov, Phys. Rev. Lett. 98, 176101 (2007)]. By permission of the American Physical Society.

The results shown above suggest a novel mechanism of transformation of monolayer to multilayer islands which differs from the ordinary layer-by-layer growth described above. An  $X$ -layer island will form by the formation and lateral, two-dimensional growth of an  $(X-1)$ -layer island. Figure 17 shows the transformation curves of mono- to three-layer islands by formation and lateral growth of bilayer island. Two curves are shown, for misfits of  $-7\%$  and  $-12\%$ . Atoms are detached from the edges of the initial monolayer island and are incorporated into the double steps of the bilayer island growing on top. The low-misfit curve is similar to the layer-by-layer curve shown in Fig. 12(b). The energy tends to increase all the way and shows at the very end a sudden collapse due to the disappearance of the single and double steps to produce low-energy facets. In the case of larger misfit (larger strain energy per bond) the curve shows a nucleation behavior. The bilayer nucleus  $i^*$  consists of 22 atoms.

In order to better understand the multilayer mode of 2D-3D transformation, let us consider it in more detail. We consider for simplicity the mono-bilayer transformations. The physics of the transformation of mono- to multilayer island is essentially the same. During the process of transformation the overall step length increases; the step length of the lower island decreases and that of the upper island increases in such a way that the total step length increases. This can be easily shown assuming square or circular islands. The variation of the step length is very important since strain is relaxed at the steps. Another effect associated with the increase of the

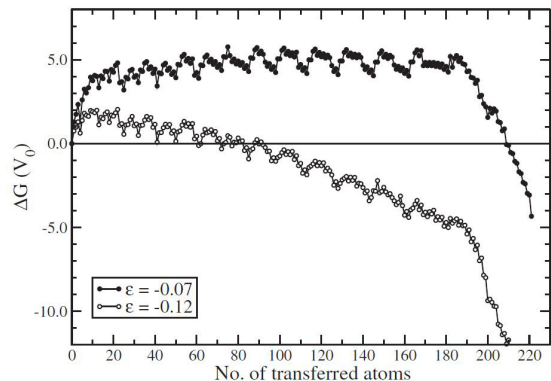


FIG. 17. Curves showing the energy change of transformation from 1 to 3 layers high islands in units of the bond energy  $V_0$  as a function of the number of atoms transferred to the upper level. Upper curve:  $f = -7\%$ , lower curve:  $f = -12\%$ . The number of atoms in the initial monolayer island ( $365 \approx 19 \times 19$ ) gives a complete truncated three-layer pyramid ( $12 \times 12 + 11 \times 11 + 10 \times 10$ ) and  $\mu = 2\nu = 26$ . (J. E. Prieto, I. Markov, Phys. Rev. Lett. 98, 176101 (2007)). By permission of the American Physical Society.

step length is the increase of the step energy since the number of the dangling bonds increases. In addition, the vertical displacements of the atoms at the steps lead to an increase of the wetting parameter, in other words, of the tendency to 3D islanding. Still another effect is the step repulsion energy, which increases as  $l^{-2}$ , where  $l$  is the step separation.[84] This plays a significant role only near the end of the transformation. The strain relaxation and the vertical displacements of the atoms close to the step edges favor the process of 3D islanding, i.e. the mono-bilayer transformation.[58, 59] The increase of the step energy and the step-step repulsion oppose it. Then, in order 3D islands to form it is necessary the first two factors to prevail. If the misfit is negative and the film material is soft (small value of the force constant  $\gamma$ ) the second layer nucleus must be thicker in order to give rise to an effectively larger value of  $\gamma$  and in turn to greater vertical displacements.

Once a pyramid of height  $X$  MLs is formed, it can continue to grow further in height by the formation and growth of monolayer nuclei. It is thus of interest to study the formation of 2D nuclei on the upper surface of the pyramid. Figure 18 shows a comparison of the nucleation barrier of mono-three-layer (1-3) transformation with the barrier for monolayer nucleation on top of the three-layer pyramid (3-4 transformation). The monotonic decrease of the nucleation barrier with misfit for the 1-3-ML transformation is characteristic of nucleation behavior.[58] The barrier for the 3-4-ML transformation is smaller than for 1-3-ML at small misfits. This means that if a 1-3 transformation takes place, a fourth layer can be formed on top. On the contrary, at larger absolute values of the misfit, the barrier for formation of a nucleus on

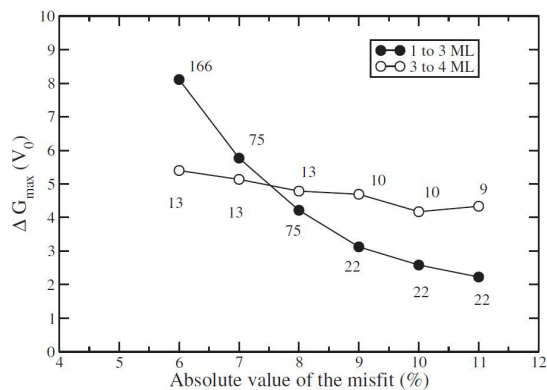


FIG. 18. Nucleation barriers in units of  $V_0$  as a function of the absolute value of the negative misfit, for transformation from single monolayer to three-layer islands. The number of atoms in the critical nucleus is given at each point. The barrier for monolayer nucleation on top of the three-layer island is also shown. The total number of atoms is 365, and  $\mu = 2\nu = 26$ . (J. E. Prieto, I. Markov, Phys. Rev. Lett. 98, 176101 (2007)). By permission of the American Physical Society.

the top surface of the three-layer pyramid is significantly greater than the barrier for formation of a bilayer nucleus on the first layer, so that the growth of the 4th atomic level might be strongly inhibited for kinetic reasons. If this is the case the multilayer pyramid will grow laterally keeping its height constant. Adatoms from the surface will prefer to join the side walls instead of nucleate on the smooth top surface. This is more important for tensile islands than for compressed ones.

## COMPARISON WITH EXPERIMENT

In this section we verify two predictions of the model, the existence of a critical misfit below which coherent 3D islands cannot be formed on the stable wetting layer, and the existence of multilayer transformation of monolayer into 3D islands.

### Critical misfit for coherent Stranski-Krastanov growth

As shown in Figs. 8 and 10, coherent 3D islands can be formed on the stable wetting layer only at misfits larger than a critical misfit  $f_{cr}$  particularly in compressed overlayers. In the important cases of Ge/Si[85, 86] and InAs/GaAs[87, 88], the overlayer is compressed by 4% and 7%, respectively. In fact, the critical misfit for monolayer transformation and its dependence on misfit sign was first suggested on the base of computer simulations on a (1+1)D model by Korutcheva *et al.*[30]

Xie *et al.*[89] found a critical compressive misfit of 1.4%

for 3D islanding upon deposition of  $\text{Si}_{0.5}\text{Ge}_{0.5}$  films on relaxed buffer layers of  $\text{Si}_x\text{Ge}_{1-x}$  varying  $x$  from 0 (pure Ge) to 1 (pure Si). In this way they covered the whole range of misfit from -2% to 2%. Films under tensile misfit were found always stable against 3D islanding.

Pinczolits *et al.*[90] have found that upon deposition of  $\text{PbSe}_{1-x}\text{Te}_x$  on  $\text{PbTe}(111)$  the overlayer remains purely two-dimensional when the misfit is less than 1.6% in absolute value (Se content < 30%). Note that contrary to the systems Ge/Si and InAs/GaAs, the lattice misfit of the system  $\text{PbSe}/\text{PbTe}$  is tensile (-5.3%). One should have in mind, however, that  $\text{PbSe}$  could be considered as a “stiff” material.[91]

Leonard *et al.* [92] have successfully grown coherent 3D islands of  $\text{In}_x\text{Ga}_{1-x}\text{As}$  on  $\text{GaAs}(001)$  with  $x = 0.5$ , or  $f \approx 3.6\%$  but 60 Å thick 2D smooth planar films at  $x = 0.17$  ( $f \approx 1.2\%$ ). Thus a critical misfit between 1.2% and 3.6% should exist.

The above result has been confirmed by Walther *et al.*[93] who found that a critical misfit of about 1.8% has to be exceeded in order 3D islands to grow in the Stranski-Krastanov mode, or a critical In content of approximately  $x = 0.25$  to be exceeded in order  $\text{In}_x\text{Ga}_{1-x}\text{As}$  quantum dots to grow on top of the wetting layer on  $\text{GaAs}(001)$ .

It is interesting to note that the critical misfit for 3D islanding to take place covers a great part of the maximal misfit of the respective system. Thus it varies from 0.25% for InAs/GaAs (1.8% from 7.2%) to 0.33% for Ge/Si (1.4% from 4.2%). The latter means that the layer-by-layer growth cannot be considered as a rare event as was thought before. This behavior of the systems studied and in particular the existence of a critical misfit cannot be explained either by the nucleation theory of 3D islands formation or by the barrierless concept.

### Forbidden island heights in strained heteroepitaxy

The last two decades have witnessed intensive studies of epitaxial growth of metals in particular Pb, Ag and Al, on semiconductors surfaces at low temperatures (130 - 180 K).[94–97] Flattop Pb islands with a preferred height of 7 monolayers were observed to grow on the wetting layer on  $\text{Si}(111)7 \times 7$ . [94–96, 98] These observations were explained in terms of the energy decrease owing to electron confinement and spilling of charge over the metal-semiconductor interface or a “quantum size effect” (QSE) by Zhang *et al.*, who coined for this reason the term “electronic growth”. [99] The thickness of islands was found to be in the range of four to nine atomic layers; among these islands, those with a height of seven ML were clearly observed to dominate; Pb islands on  $\text{Si}(111)$  with thicknesses ranging from 1 to 3 MLs were never observed.[96, 100, 101] Flattop islands with a preferred height grow laterally without thickening.[94, 101, 102]

It was also observed that 2-ML thick flattop Ag islands on Si(111) increase linearly in size preserving their height,[94] whereas single layer islands preserve a nearly constant size of 500Å.[103]

The above observations can be explained by the quantum size effect, but we show that classical effects associated with strain relaxation at steps and the interplay of strain and edge energies can give a plausible explanation as well.[82]

Obviously, the first thing to do is to estimate the strain energy per bond  $\mathcal{E}$  for the metals under study in the experiments Pb, Ag and Al. For this aim we need an estimate of the respective force constant by making use of the relation  $\gamma = Eb/2(1 + \mu_P)$  where  $E$  and  $\mu_P$  are the Young modulus and the Poisson ratio of the overlayer material. We get the values 0.15, 3.08 and 2.27 in units of  $V_0$  for Pb, Ag and Al, respectively. With a value of 0.15 for Pb we expect a transition from 1 to 8-9 MLs in reasonable agreement with the experimental value of preferred height of 7 MLs.[94–96, 98, 100, 101, 103]

The very high values of  $\mathcal{E}$  estimated for Ag and Al are due to the expected failure of the harmonic approximation for high values of the misfit. Anyway the prediction is the presence of thinner islands, as observed in experiment.[103, 104] Note that our estimations are performed on coherent islands with (100) orientation, while most experiments are performed on Si(111). However, our estimations should be approximately valid, because the relaxation of the strain energy must be partially balanced by disregistry.

The lateral growth of 2-ML high Ag islands until coalescence[94] can be explained by inhibited nucleation of 2D islands on top of the bilayer islands. The constant size of 500Å of the monolayer islands observed experimentally[103] can be considered as the critical size  $N_{12}$ . Clear evidence for a transformation process is the rearrangement of 2- to 3-ML high Fe islands on Cu<sub>3</sub>Au(001) deposited at 140 K when annealed at 400 K.[105, 106]

Finally, based on the above considerations, we predict that soft tensile metal overlayers should undergo a multilayer transformation whereas stiffer compressed metals overlayers should show a layer-by-layer transformation. Thus we can expect that In with  $\mathcal{E} = 0.17V_0$  should undergo a multilayer transformation similar to that of Pb/Si(111) but with a slightly smaller preferred height. Indeed, Chen *et al.* observed the formation of flattop In islands with a preferred height of 4 MLs.[107]

## DISCUSSION

As follows from the discussion above, Bauer’s criterion of wettability of the substrate by the overlayer material can be successfully applied to the Stranski-Krastanov growth mode. We will show that the idea of the trade-

off of the strain relaxation energy and the surface energy does not contradict the concepts developed in this paper. We do not discuss the barrierless transformation of ripples as one possible additional mechanism of formation of 3D islands.

The trade-off between strain and surface energies is a macroscopic concept. The development of an effective positive wetting parameter owing to the lattice misfit is a microscopic phenomenon. If we assume that the stable wetting layer grows in a layer-by-layer mode by the formation and lateral spreading of 2D nuclei, it is logical to suppose that further deposition will proceed in the same way. The resulting 2D islands are enclosed by step edges. Strain relaxation takes place at these steps. Atoms at the edges are displaced from their positions in the bottoms of the corresponding potential troughs and the atomic separations at the edges and corners of the islands are very close to the natural separation of the bulk deposit crystal. For this reason the nucleation of the second layer takes often place at the edges and corners as “...atoms are happy to be there, because they find an atomic distance they would like to have”,[108](see also Ref. (109)). Experimental evidence supports this conclusion.[110–112]

The smaller the misfit, the smaller the displacements of the edge atoms and in turn, the stronger is the average wetting (the smaller is the effective wetting parameter). This leads to the appearance of a critical misfit below which the wetting parameter is too small and the energy of the bilayer islands is always larger than that of the monolayer ones (see Fig. 9). The curves of the energies of mono- and bilayer islands do not cross each other. The formation of coherent 3D islands becomes thermodynamically unfavored. The film will continue to grow in a 2D mode until the strain is relaxed by the introduction of misfit dislocations. In order for the mono- and bilayer islands energies to cross each other to give rise to 3D islanding, the misfit and in turn the strain relaxation at the edges must be larger.

We conclude from the above consideration that the critical misfit,  $f_{cr}$ , represents in fact the dividing line between the FM and SK growth modes. We then can devise a phase diagram for the occurrence of any mode of growth in coordinates wetting parameter - lattice misfit (see Fig. 19). Volmer-Weber mode of growth takes place at positive values of the wetting parameter. The curve slightly decreases with increasing misfit thus widening the field for VW growth because of the contribution of the misfit to the wetting as discussed above. Both FM and SK modes take place below this line, FM at misfits smaller than the critical misfit and the SK mode at larger values of the misfit. Note that in tensile overlayers the dividing line between the FM and SK modes should be placed at greater absolute values of the misfit. This phase diagram differs from the one suggested by Grabow and Gilmer[72] by the displacement of the FM growth from zero misfit to the critical misfit,  $f_{cr}$ , as discussed

above. Note that in our case  $f_{cr}$  can be larger or smaller depending on the misfit sign, and more importantly, on the material stiffness. In the case of very soft materials and negative misfits,  $f_{cr}$  can be so large that Stranski-Krastanov growth may not take place at all. It is noteworthy that the critical misfit in alloy films could reach a significant value of about 30% of the misfit between the pure binaries (Ge/Si or InAs/GaAs).

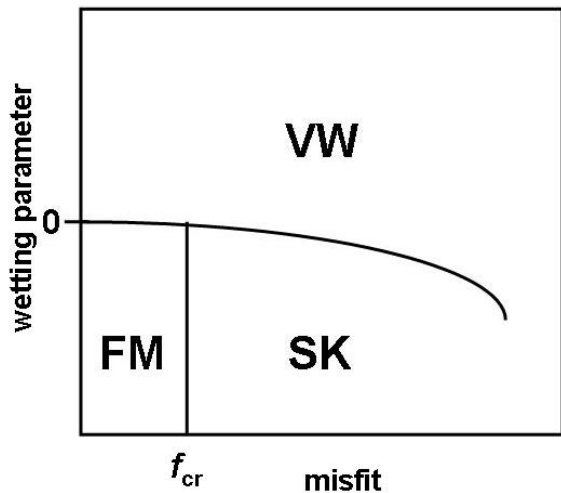


FIG. 19. Schematic representation of the phase diagram for the occurrence of the VW, FM and SK growth modes.

The average adhesion (the wetting) depends strongly on the anharmonicity of the interatomic forces. Tensile islands adhere more strongly to the wetting layer and the critical misfit beyond which coherent 3D islanding is possible is much larger in absolute than in compressed overlayers. As a result, coherent SK growth in tensile films could be expected at very (sometimes unrealistically) large absolute values of the negative misfit. The critical misfit, however, depends on the material parameters (degree of anharmonicity, strength of the chemical bonds, etc.) of the particular system and the formation of coherent quantum dots in tensile overlayers cannot be completely ruled out.

The weaker average adhesion in compressed overlayers leads to another effect at misfits larger than the critical one. Owing to the stronger interatomic repulsive forces, the edge atoms in compressed monolayer islands adhere weaker to the wetting layer compared to expanded islands. This results in an easier transformation of mono- to bilayer islands, which is the first step to the complete 2D-3D transformation. The latter includes also kinetics in the sense that the edge atoms have to detach and form the upper layers. However, it is not the strain at the edges (which is nearly zero) that is responsible for the easier detachment of the edge atoms as suggested by Kandel and Kaxiras[113] but the weaker adhesion. The 2D-3D transformation is hindered in tensile overlayers as the edge atoms adhere more strongly to the wetting layer.

On the other hand, the existence of such critical sizes, which determine the intervals of stability of islands with different thicknesses, could be considered as the thermodynamic reason for the narrow size distribution of 3D islands which is observed in experiments. This does not mean that this is the only reason. Elastic interactions between islands and growth kinetics can have stronger effects than thermodynamics. The 2D-3D transformation takes place by consecutive nucleation events, each one needing to overcome a lower energetic barrier than the preceding one. Thus, the mono-bilayer transformation appears as the rate-determining step. This is easy to understand. Thicker islands have larger values of the wetting function which facilitates the transformation from  $X$  to  $X + 1$  MLs high islands.

We conclude that the criterion of Bauer describes well the transition from planar growth to 3D islanding in the Stranski-Krastanov growth mode as a transition from the FM to the VW growth mode. The only difference from the classical VW growth is that in the latter the adhesion parameter is constant and is due to difference in chemical bonding. In the case of the coherent SK mode the chemical bonding is the same and the nonzero adhesion parameter is due to the misfit and depends on the island thickness.

Let us now try to answer the question asked in the Introduction. As discussed above, the driving force for the 3D island formation is the relaxation of elastic stress: the island nucleates because the elastic energy per atom in the wetting layer is larger than in the island. The relaxation of the strain in 3D islands with respect to the wetting layer overcompensates the surface energy of the side facets of the 3D crystallites. This is the main idea of the nucleation concept. However, the elastic stress in the initial 2D islands on top of the wetting layer gives rise to a positive effective wetting parameter. The latter is the thermodynamic driving force for 3D islanding in the sense of the wettability criterion of Bauer. We conclude that the 3D islanding in SK growth mode obeys the criterion of Bauer owing to the particular structure of the interface between the stable wetting layer and the 2D islands on top which appear as precursors of the 3D crystallites.[4, 5]

In summary, we conclude that the Stranski-Krastanov growth mode appears as a sequence of Frank-van der Merwe and Volmer-Weber growth modes. The wetting layer and the 3D islands represent different phases in the sense of Gibbs which cannot be in equilibrium with each other. The separate monolayers which belong to the wetting layer represent also different phases which have different equilibrium vapor pressures. Monolayer-high islands with a critical size appear as necessary precursors for 3D islands. The 2D-3D transition takes place through a series of intermediate states with discretely increasing thickness that are stable in separate intervals of volume in the case of “stiff” materials or by the formation and lateral growth of 2D multilayer nuclei in the

case of “soft” materials like Pb and In. At sufficiently large misfits, the barrier for 2D multilayer nucleation is significantly smaller than the barrier for the subsequent single-layer nucleation. Then islands with a preferred height will continue to grow laterally instead of growing in height. There exists a critical misfit below which coherent 3D islands are thermodynamically unfavored and the misfit is accommodated by misfit dislocations at a later stage of growth. Coherent 3D islands can only form at misfits larger in absolute value than the critical misfit. Compressed overlayers show a greater tendency to 3D clustering than expanded ones, in agreement with experimental results. The mechanism of the layer-by-layer transformation in compressed overlayers is nucleation-like due to the interplay of relaxation of the in-plane strain, which is proportional to the total edge length and the increase of the total edge energy and the repulsion between the edges. The critical nucleus consists of one atom in addition of a compact shape; it plays the role of a one-dimensional nucleus giving rise to a new atomic row. The compact shape is in general a rectangle with edges of  $i$  and  $i - 1$  atoms, while square shapes can also appear if the length of the critical nucleus is comparable to the number of atoms in the edge of the original first-layer island. In some cases nuclei in the upper layer can form on the edges or the corners of the underlying 2D island as the atom separations there are nearly the same as in the bulk deposit crystal. The transformation curve in tensile overlayers shows a “non-nucleation” behavior characterized by an overall increase of the energy up to the stage when the single steps coalesce to produce low-energy facets. This is accompanied by a collapse of the energy.

This research did not receive any specific grant from funding agencies in the public, commercial or not-for-profit sectors.

---

\* joseemilio.prieto@uam.es; imarkov@ipc.bas.bg

- [1] E. Bauer, *Z. Kristallogr.* **110**, 372 (1958).
- [2] R. Kern, G. LeLay, and J. J. Metois, *Current Topics in Materials Science* **3**, ed. E. Kaldis, (North Holland, 1979), p. 128.
- [3] M. Volmer and A. Weber, *Z. phys. Chem.* **119**, 277 (1926).
- [4] F. C. Frank and J. H. van der Merwe, *Proc. Roy. Soc. London A* **198**, 205 (1949).
- [5] F. C. Frank and J. H. van der Merwe, *Proc. Roy. Soc. London A* **198**, 216 (1949).
- [6] I. N. Stranski und L. Krastanov, *Sitzungsber. Akad. Wissen. Wien* **46**, 797 (1939).
- [7] R. Kaischew, *Commun. Bulg. Acad. Sci. (Phys.)* **1**, 100 (1950).
- [8] R. Kaischew, *Fortschr. Miner.* **38**, 7 (1960).
- [9] I. Markov. *Crystal Growth for Beginners, Fundamentals of Nucleation, Crystal Growth and Epitaxy*, 3rd edition, World Scientific, Singapore, 2017.
- [10] R. Peierls, *Phys. Rev. B* **18**, 2013 (1978).
- [11] J. Tersoff and R.M. Tromp, *Phys. Rev. Lett.* **70**, 2782 (1993).
- [12] J. Tersoff and F.K. LeGoues, *Phys. Rev. Lett.* **72**, 3570 (1994).
- [13] P. Politi, G. Grenet, A. Marty, A. Ponchet, and J. Villain, *Phys. Rep.* **324**, 271 (2000).
- [14] D. J. Eaglesham and M. Cerullo, *Phys. Rev. Lett.* **64**, 1943 (1990).
- [15] Y.-W. Mo, D. E. Savage, B. S. Swartzentruber, and M. G. Lagally, *Phys. Rev. Lett.* **65**, 1020 (1990).
- [16] E. Sutter, P. Sutter, and J. E. Bernard, *Appl. Phys. Lett.* **84**, 2262 (2004).
- [17] M. A. Lutz, R. M. Feenstra, P. M. Mooney, J. Tersoff, and J. O. Chu, *Surf. Sci.* **316**, L1075 (1994).
- [18] M. Brehm, H. Lichtenberger, T. Fromherz, and G. Springholz, *Nanoscale Res. Lett.* **6**, 70 (2011).
- [19] C. Teichert, *Phys. Rep.* **365**, 335 (2002).
- [20] J. Tersoff, C. Teichert, and M. Lagally, *Phys. Rev. Lett.* **76**, 1675 (1996).
- [21] K. M. Chen, D. E. Jesson, S. J. Pennycook, T. Thundat, and R. J. Warmack, *Phys. Rev. B* **56**, R1700 (1997).
- [22] A. Vailionis, B. Cho, G. Glass, P. Desjardins, D. G. Cahill, and J. E. Greene, *Phys. Rev. Lett.* **85**, 3672 (2000).
- [23] P. Sutter and M. G. Lagally, *Phys. Rev. Lett.* **84**, 4637 (2000).
- [24] R. J. Asaro and W. A. Tiller, *Metall. Trans.* **3**, 1789 (1972).
- [25] M. A. Grinfeld, *Sov. Phys. Dokl.* **31**, 831 (1986).
- [26] D. J. Srolovitz, *Acta Metall.* **37**, 621 (1989).
- [27] A. Pimpinelli and J. Villain, *Physics of Crystal Growth*, (Cambridge University Press, 1998).
- [28] R. M. Tromp, F. M. Ross, and M. C. Reuter, *Phys. Rev. Lett.* **84**, 4641 (2000).
- [29] J. Tersoff, B. J. Spencer, A. Rastelli, and H. von Känel, *Phys. Rev. Lett.* **89**, 196104 (2002).
- [30] E. Korutcheva, A.M. Turiel, and I. Markov, *Phys. Rev. B* **61**, 16890 (2000).
- [31] Ch. Ratsch, and A. Zangwill. *Surf. Sci.* **293**, 123 (1993).
- [32] J. H. van der Merwe, *Surf. Sci.* **449**, 151 (2000).
- [33] S. A. Kukushkin, A. V. Osipov, F. Schmitt, and P. Hess, *Semiconductors* **36**, 1097 (2002).
- [34] P. P. Petrov, and W. Miller, *Comp. Mater. Sci.* **60**, 176 (2012).
- [35] M. Biehl, M. Ahr, W. Kinzel, and F. Much, *Thin Solid Films* **428**, 52 (2003).
- [36] K. E. Khor, and S. Das Sarma. *Phys. Rev. B* **62** 16657 (2000).
- [37] A. R. Avery, H. T. Dobbs, D. M. Holmes, B. A. Joyce, and D. D. Vvedensky, **79**, 3938 (1997).
- [38] P. Ashu, and C. C. Matthai. *Appl. Surf. Sci.* **48**, 39 (1991).
- [39] Ch. Roland, and G. H. Gilmer. *Phys. Rev. B* **47** 16286 (1993).
- [40] B. A. Joyce, J. L. Sudijono, J. G. Belk, H. Yamaguchi, X. M. Zhang, H. T. Dobbs, and T. S. Jones, *Jap. J. Appl. Phys.* **36**, 4111 (1997).
- [41] J. L. Xu, and J. Y. Feng. *Nuclear Instruments and Methods in Physics Research Section B: Beam Interactions with Materials and Atoms* **217** 33 (2004).
- [42] V. G. Dubrovskii, *Nucleation theory and growth of nanostructures*, (Springer-Verlag Berlin Heidelberg



- 2014).
- [43] V.A. Shchukin, D. Bimberg, *Rev. Mod. Phys.* **71**, 1125 (1999).
- [44] V.A. Shchukin, N.N. Ledentsov, D. Bimberg, *Epitaxy of Nanostructures*, (Springer, New York, 2003).
- [45] A. Bhattacharya and B. Bansal, *Handbook of Crystal Growth, Vol. 3, 2nd Edition*, Ed T. Kuech, (Elsevier 2015), pp. 1057-1099.
- [46] I. N. Stranski, *Z. phys. Chem.* **A 142**, 453 (1929).
- [47] I. N. Stranski und K. Kuleliev, *Z. phys. Chem.* **A 142**, 467 (1929).
- [48] W. Kossel, *Nachrichten der Gesellschaft der Wissenschaften Göttingen, Mathematisch-Physikalische Klasse, Band 135*, 1927.
- [49] I. N. Stranski, *Ann. l'Univ. Sofia* **24**, 297 (1927).
- [50] I. N. Stranski, *Z. phys. Chemie* **36**, 259 (1928).
- [51] R. Kaischew, *J. Cryst. Growth* **51**, 643 (1981).
- [52] J. E. Prieto and I. Markov, *Phys. Rev. B* **66**, 073408 (2002).
- [53] J. W. Gibbs, *On the equilibrium of heterogeneous substances, Collected works*, (Longmans, Green & Co., 1928).
- [54] I. Markov and A. Milchev, *Surf. Sci.* **136**, 519 (1984).
- [55] I. Markov and A. Milchev, *Surf. Sci.* **145**, 313 (1984).
- [56] I. Markov, *Phys. Rev. B* **48**, 14016 (1993).
- [57] J. Tersoff, *Phys. Rev. Lett.* **56**, 632 (1986).
- [58] J. E. Prieto and I. Markov, *Phys. Rev. B* **72**, 205412 (2005).
- [59] P. Müller and R. Kern, *Appl. Surf. Sci.* **102**, 6 (1996).
- [60] J. G. Dash, *Phys. Rev. B* **15**, 3136 (1977).
- [61] B. Mutaftschiev, *The Atomistic Nature of Crystal Growth*, Springer Series in Materials Science, Vol. 43, 2001.
- [62] S. Stoyanov and I. Markov, *Surf. Sci.* **116**, 313 (1982).
- [63] C. Priester and M. Lannoo, *Phys. Rev. Lett.* **75**, 93 (1995).
- [64] Y. Chen and J. Washburn, *Phys. Rev. Lett.* **77**, 4046 (1996).
- [65] B. Voigtländer and A. Zinner, *Appl. Phys. Lett.* **63**, 3055 (1993).
- [66] Y. Ebiko, S. Muto, D. Suzuki, S. Itoh, H. Yamakoshi, K. Shiramine, T. Haga, K. Unno, and M. Ikeda, *Phys. Rev. B* **60**, 8234 (1999).
- [67] D. Walton, in: *Nucleation*, ed. by A. G. Zettlemoyer, (Marcel Dekker, 1969), p. 370.
- [68] I. Markov and S. Stoyanov, *Contemp. Phys.* **28**, 267 (1987).
- [69] R. Xiang, M. T. Lung, and C.-H. Lam, *Phys. Rev. B* **82**, 021601 (2010).
- [70] D. Kashchiev, *Nucleation, Basic Theory with Applications*, Butterworth - Heinemann, Oxford, 2000.
- [71] I. Markov, in *Springer Handbook of Crystal Growth*, edited by G. Dhanaraj, K. Byrappa, V. Prasad, and M. Dudley, (Springer, Berlin, 2010), p. 17.
- [72] M. Grabow and G. Gilmer, *Surf. Sci.* **194**, 333 (1988).
- [73] H. Sunamura, N. Usami, Y. Shiraki, S. Fuketsu, *Appl. Phys.* **66**, 3024 (1995).
- [74] A. Grimm, A. Fissel, E. Bugiel, T. F. Wiefler, *Appl. Surf. Sci.* **340**, 40 (2016).
- [75] G. Saint-Girous, G. Patriarche, A. Merenta, I. Sagues, *J. Appl. Phys.* **91**, 3859 (2002).
- [76] J. M. Moison, F. Houzay, F. Barthe, L. Leprince, E. André, and O. Vatel, *Appl. Phys. Lett.* **64**, 196 (1994).
- [77] V. Borge, F. Hassen, H. Maaref, J. Dazard, Y. Monteil, J. Davenas, *Microelectr. J.* **30**, 347 (1999).
- [78] D. Kashchiev, *J. Chem. Phys.* **129**, 164701 (2008).
- [79] V. V. Voronkov, *Sov. Phys. Crystallogr.* **15**, 13 (1970).
- [80] F. C. Frank, *J. Cryst. Growth* **22**, 233 (1974).
- [81] J. Zhang and G. H. Nancollas, *J. Cryst. Growth* **106**, 181 (1990).
- [82] J. E. Prieto and I. Markov, *Phys. Rev. Lett.* **98**, 176101 (2007).
- [83] J. H. van der Merwe, J. Woltersdorf, and W. A. Jesser, *Mater. Sci. Eng.* **81**, 1 (1986).
- [84] P. Nozières, in *Solids Far from Equilibrium*, edited by C. Godrèche (Cambridge University Press, Cambridge, England, 1992), p. 1.
- [85] B. Voigtländer, *Surf. Sci. Rep.* **43**, 127 (2001).
- [86] D. J. Eaglesham and R. Hull, *Mater. Sci. Eng. B* **30**, 197 (1995).
- [87] B. A. Joyce and D. D. Vvedensky, *Mater. Sci. Eng. Rep.* **46**, 127 (2004).
- [88] J. Wu and P. Jin, *Front. Phys.* **10**, 108101 (2015).
- [89] Y. H. Xie, G. H. Gilmer, C. Roland, P. J. Silverman, S. K. Buratto, J. Y. Cheng, E. A. Fitzgerald, A. R. Kortan, S. Schuppler, M. A. Marcus, and P. H. Citrin, *Phys. Rev. Lett.* **73**, 3006 (1994).
- [90] M. Pinczolit, G. Springholz, and G. Bauer, *Appl. Phys. Lett.* **73**, 250 (1998).
- [91] J. E. Petersen, L. M. Scolfaro, and T. H. Myers, *Mater. Chem. Phys.* **146**, 472 (2014).
- [92] D. Leonard, M. Krishnamurthy, C.M. Reaves, S.P. Denbaars, and P.M. Petroff, *Appl. Phys. Lett.* **63**, 3203 (1993).
- [93] T. Walther, A.G. Cullis, D.J. Norris, and M. Hopkinson, *Phys. Rev. Lett.* **86**, 2381 (2001).
- [94] L. Gavioli, K. R. Kimberlin, M. C. Tringides, J. F. Wendelken, and Z. Zhang, *Phys. Rev. Lett.* **82**, 129 (1999).
- [95] M. Hupalo, V. Yeh, L. Berbil-Bautista, S. Kremmer, E. Abram, and M. C. Tringides, *Phys. Rev. B* **64**, 155307 (2001).
- [96] W. B. Su, S. H. Chang, W. B. Jian, C. S. Chang, L. J. Chen, and Tien T. Tsong, *Phys. Rev. Lett.* **86**, 5116 (2001).
- [97] L. Floreano, D. Cvetko, F. Bruno, G. Bavdek, A. Cosaro, R. Gotter, A. Verdini, and A. Morgante, *Prog. Surf. Sci.* **72**, 135 (2003).
- [98] V. Yeh, L. Berbil-Bautista, C. Z. Wang, K. M. Ho, and M. C. Tringides, *Phys. Rev. Lett.* **85**, 5158 (2000).
- [99] Z. Zhang, Q. Niu, and C.-K. Shih, *Phys. Rev. Lett.* **80**, 5381 (1998).
- [100] S. H. Chang, W. B. Su, W. B. Jian, C. S. Chang, L. J. Chen, and Tien T. Tsong, *Phys. Rev. B* **65**, 245401 (2002).
- [101] M. M. Özer, Y. Jia, B. Wu, Z. Zhang, and H. H. Weitering, *Phys. Rev. B* **72**, 113409 (2005).
- [102] K. Budde, E. Abram, V. Yeh, and M. C. Tringides, *Phys. Rev. B* **61**, 10602(R) (2000)
- [103] W. B. Su, H. Y. Lin, Y. P. Chiu, H. T. Shih, T. Y. Fu, Y. W. Chen, C. S. Chang, and Tien T. Tsong, *Phys. Rev. B* **71**, 073304 (2005).
- [104] H. Liu, Y.F. Zhang, D.Y. Wang, M.H. Pan, J.F. Jia, and Q.K. Xue, *Surf. Sci.* **571**, 5 (2004).
- [105] M. Canepa, P. Cantini, C. Mannori, S. Terreni, and L. Mattera, *Phys. Rev. B* **62**, 13121 (2000)
- [106] A. Verdini, L. Floreano, F. Bruno, D. Cvetko, A. Morgante, F. Bisio, S. Terreni, and M. Canepa, *Phys. Rev.*

- B **65**, 233403 (2002).
- [107] J. Chen, M. Hupalo, M. Ji, C. Z. Wang, K. M. Ho, and M. C. Tringides, Phys. Rev. B **77**, 233302 (2008).
- [108] J. Villain, J. Cryst. Growth **275**, e2307 (2005).
- [109] J. E. Prieto and I. Markov, Phys. Rev. B **84**, 195417 (2011).
- [110] J. Shi and X. R. Qin, Phys. Rev. B **73**, 121303(R) (2006).
- [111] P. W. Murray, I. Stensgaard, E. Laegsgaard, and F. Besenbacher, Phys. Rev. B **52**, R14404 (1995).
- [112] S. I. Molina, M. Varela, D. L. Sales, T. Ben, J. Pizarro, P. L. Galindo, D. Fuster, Y. González, L. González, and S. J. Pennycook, Appl. Phys. Lett. **91**, 143112 (2007).
- [113] D. Kandel and E. Kaxiras, Phys. Rev. Lett. **75**, 2742 (1995).